International Journal of Advanced Research in Physical Science (IJARPS)
Volume 6, Issue 1, 2019, PP 1-6
ISSN No. (Online) 2349-7882
www.arcjournals.org

The Spectroscopic Studies of CdS Nanofibers Synthesized via Dc-Sputtering Technique

P. K. Ghosh

Department of Physics, Abhedananda Mahavidyalaya, Sainthia, Birbhum, W.B, India

Corresponding Author:** ***P. K. Ghosh, *Department of Physics, Abhedananda Mahavidyalaya, Sainthia,*

Abstract: *The field emission property of transparent CdS nanofibers, grown by direct current-sputtering technique on Si and glass substrates, has been studied without using any catalyst or matrix. X-ray diffraction patterns and selected area electron diffraction patterns confirmed the cubic CdS phase formation in the thin films although the initial target material was hexagonal CdS powder. TEM micrographs have confirmed the nanofiber formation with diameters in the range 2 - 4.3 nm and length a few microns. XRD patterns showed the crystal size increased with the increase of deposition time. The Fowler-Nordhiem plots of the emission current from the nano-CdS thin films are almost straight line. The turn-on fields of the grown nano-CdS thin films are found to be in the range 3.6 - 6.6 V/μm. Only bulk-CdS thin film grown on Si substrates have not showed field emission property under the same conditions.*

Keywords: *CdS nanofibres; dc-sputtering; nanostructural; optical, field emission*

1. INTRODUCTION

The unconventional properties of nanostructured materials have recently attracted tremendous interest because of their potential uses in both mesoscopic research and the development of nanodevices [1]. The electron field emission exhibited by nanometer-sized materials is one of the most attractive properties for practical applications [2]. It is known that the macroscopically flat surfaces emit electrons at macroscopic field values considerably less than the local field at which cold electron emission normally takes place [3]. This phenomenon of low-macroscopic-field emission [4] is of great technological interest in vacuum microelectronics and field emission displays.

Recently, various research groups are working on many new kind of materials which are appropriate for field emitters for possible application in near future. However, semiconductor nanocrystals have attracted much interest during the last decade because of their interesting properties. Transparent nanostructured CdS thin films have received much attention for several practical applications [5]. The field emission properties of many transparent semiconductors like ZnO [6], $CuAlO_2$ [7] etc. have been studied widely. Jia et al [8] and Chen et al [9] have also reported the field emission from In_2O_3 and Cu_2S respectively. Previously, the field emission from CdS/SiO_2 nanocomposites and nano-CdS modified porous silicon have been reported by Jiao et al [10] and Ling et al [11] respectively. In this Paper, we have reported the detailed studies of effect electrode distance on field emission properties of cadmium sulphide nanofibers, grown by direct current-sputtering technique on Si substrates, has been studied without using any catalyst or matrix.

2. EXPERIMENTAL

2.1. Synthesis

Target of cadmium sulfide (CdS) was fabricated by taking a suitable aluminium holder (5 cm dia.) and compacting the CdS polycrystalline powder (Aldrich, purity 99.99%) by applying suitable hydrostatic pressure (~ 100 kg / cm^2). The fabricated CdS target was placed in the dc-sputtering chamber for the deposition of nanocrystalline thin films on various substrates.

The films were synthesized at room temperature and the substrates used were glass and Si. The glass substrates were cleaned at first by a mild soap solution, then in boiling water and in an ultrasonic cleaner and finally degreased in alcohol vapor. For Si substrates, to remove the surface oxide layer, they were etched in HF (~20%) for 5 minutes and finally cleaned in an ultrasonic cleaner. The chamber was evacuated by conventional rotary and diffusion pump combination to a base pressure of

10^{-6} mbar. Before starting the actual deposition the target was pre-sputtered and the substrates were covered by a movable shutter. The working pressure of the evacuated chamber was maintained at ~ 0.5 mbar by sending argon gas during deposition of the film. Sputtering was performed at 1.7 kV and corresponding current density was 3.2 mA/cm^2. The distance of the target and substrate was ~ 1.6 cm. For TEM measurement the films were scratched out carefully by a sharp knife edge from some portion of the glass substrates. These particles were dispersed in ethanol by ultrasonication and then a few drop of this solution, was placed on carbon coated copper grid and it was allowed to dry out. For different deposition time different carbon coated copper grids were used and the materials on carbon coated copper grid were utilized to measure the TEM image.

The deposited films were characterized by studying mainly structural and optical properties. UV-Vis transmittance measurement was performed by using a spectrophotometer (Hitachi U3400). For structural studies an X-ray diffractometer (Bruker D8 Advance) was used. XRD pattern was measured in the 2θ range 20 - 70 ^{o} using Cu Kα radiation (λ = 0.15406 nm). For TEM measurement a transmission electron microscope (Hitachi 600) was used.

2.2. Characterization

The deposited films were characterized by studying mainly nanostructural, optical and field emission properties. Optical transmission spectra of the films on glass substrates were measured using a UV-Vis-NIR spectrophotometer (Shimadzu UV-3101PC). The nanostructures and corresponding diffraction patterns of the films were studied by transmission electron microscope (TEM, Hitachi-H600) and XRD pattern was recorded by a X- ray diffractometer (Bruker D8 Advance). Field emission measurements were carried out by using a diode configuration consisting of a cathode (the film under test) and a stainless steel tip anode (conical shape with a 1mm tip diameter) mounted in a liquid nitrogen trapped rotary-diffusion vacuum chamber with appropriate chamber baking arrangement. The measurement was performed at a base pressure of ~7 x 10^{-7} mbar. The Ohmic nature of the contact was checked before field emission experiment. The sheet resistance of our film was few hundred mega-ohms/square and the maximum emission current measured, was almost 10 μA. So, during emission process, if any voltage drop occurred between the contact and the portion of the sample just under the anode tip, it would be at the most, of the order of few hundred millivolts, which was quite small compared to the applied voltages (~ kV). Hence we neglected this drop and all the calculations were done with the applied voltages. The tip-sample distance was continuously adjustable to a few hundred μm by spherometric arrangement with a screw-pitch of 10 μm. The tip was first touched to the sample surface and then raised by a controlled amount according to the spherometer-scale attached to the anode. The whole surface of the film was visible through the chamber view port, which enabled us to recognize the electron emission and discharge, if any. It was confirmed that no discharge was taking place between the anode and the sample, so the current detected, was entirely due to cold field-emission process.

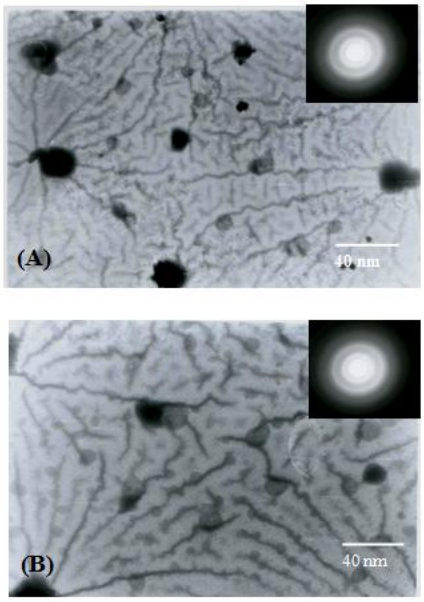

Figure1. *TEM of CdS nanofibers for deposition time (A) 10 min. and (B) 20 min., and Inset: corresponding SAED pattern of each*

3. RESULTS AND DISCUSSION

3.1. Nanostructural

The nanostructure of the films, prepared by dispersing the nanoparticles on carbon coated copper grid, have been studied by TEM as shown in Figure 1 (A) and (B), and inset of corresponding figures showed the selected area electron diffraction (SAED) patterns from which we calculated the inter-planer spacing (d) values, which correspond to reflection from (111) and (220) planes of cubic CdS. The average diameters in the range 2 - 4.3 nm and length a few microns were determined from TEM micrographs.

3.2. X- Ray Diffraction

Figure 2 (A) shows the X-ray diffraction patterns of CdS thin films deposited on Si substrates. Here we see one peak of cubic CdS due to reflection form (111) plane as in JCPDS data card [12]. Also one high intense peak appeared due to reflection from (004) plane of Si substrates.

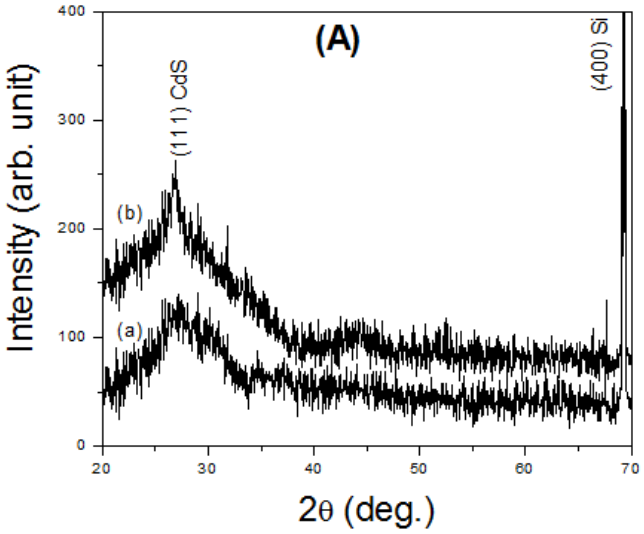

Figure2. *(A). XRD patterns of CdS thin film deposited on Si substrate for different deposition time (a) 10 min. and (b) 20 min*

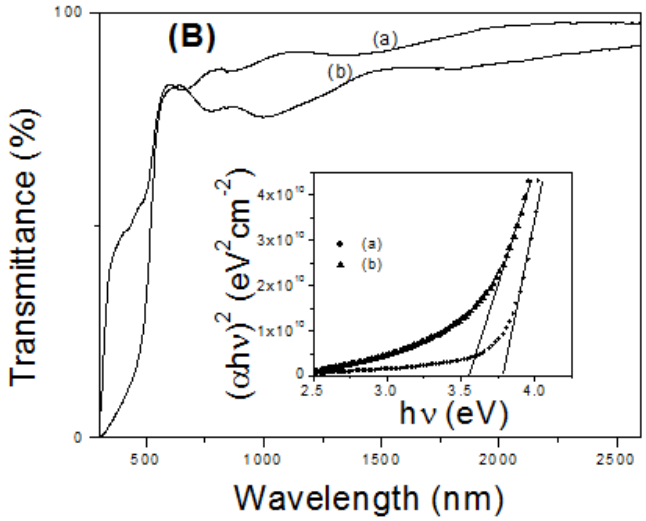

Figure2.(B). *Transmittance vs. wavelength plot of nanocrystalline CdS thin film deposited on glass substrates for different deposition time (a) 10 min. and (b) 20 min., Inset: Plot to calculate the direct bandgap of the films.*

3.3. Optical Studies

The band gap of the film E_g was determined from the transmission vs. wavelength traces as shown in Figure 2(B) for different deposition time. The relation between the absorption coefficients (α) and the incident photon energy ($h\nu$) can be written as [13],

$$(\alpha h\nu)^{1/n} = A(h\nu - E_g) \quad (1)$$

where A is a constant and E_g is the band gap of the material and exponent n depends on the type of transition. For direct allowed n = 1/2, indirect allowed transition, n = 2, and for direct forbidden, n = 3/2. To determine the possible transitions, $(\alpha h\nu)^{1/n}$ vs. hν were plotted and corresponding band gaps were obtained from extrapolating the straight portion of the graph on hν axis. The direct band gaps values of the films have been obtained from $(\alpha h\nu)^2$ vs. hν plot as shown in the inset of Figure 2(B). The direct band gaps values of the films lie in the range 3.55 - 3.76 eV.

3.4. Field Emission Studies

The applied electric fields and corresponding emission currents have been measured for different particle sizes of the films with different electrode distances. Figure 3 (A) and (B) show the emission current (I) vs. macroscopic field (E) curves of CdS thin film deposited on Si substrate with average nanofibers diameters in the range 2 - 4.3 nm and length a few microns respectively for anode-sample separation (d) of 60 μm, 80 μm and 100 μm. The macroscopic field is calculated from the external voltage applied (V), divided by the anode-sample spacing, d (obtained from our field-emission apparatus). Theoretically, the emission current I is related to the macroscopic electric field E by

$$I = Aat_F^{-2}\phi^{-1}(\beta E)^2 \exp\{\frac{-bv_F\phi^{3/2}}{\beta E}\} \quad (2)$$

where, ϕ is the local work-function, β is the field enhancement factor, A is the effective emission area, a is the First Fowler-Nordheim(F-N) Constant (1.541434 x 10^{-6} A eV V^{-2}), b is the Second F-N Constant (6.830890 x 10^9 $eV^{-3/2}$ V m^{-1}), and v_F and t_F are the values of the special field emission elliptic functions v and t [14], evaluated for a barrier height ϕ.

In so-called Fowler-Nordheim coordinates, this equation takes the form:

$$\ln\{\frac{I}{E^2}\} = \ln\{t_F^{-2}Aa\phi^{-1}\beta^2\} - \frac{(v_F b\phi^{3/2}\beta^{-1})}{E} \quad (3)$$

An experimental F-N plot is modeled by the tangent to this curve, taken in the mid-range of the experimental data. This tangent can be written in the form [15]:

$$\ln\{\frac{I}{E^2}\} = \ln\{rAa\phi^{-1}\beta^2\} - \frac{(sb\phi^{3/2}\beta^{-1})}{E} \quad (4)$$

where r and s are appropriate values of the intercept and slope correction factors, respectively. Typically, s is of the order of unity, but r may be of order 100 or greater. Both r and s are relatively slowly varying functions of 1 / E, so a F-N plot (plotted as a function of 1 / E) is expected to be a good straight line. The F-N plots of our samples are shown in Fig. 4. It has been observed that the I-E curve in the present work is closely fitted with straight line. This suggests that the electrons are emitted by cold field emission process. The turn-on field, which we define as the macroscopic field needed to get an emission current I = 0.03598 μA**,** (which corresponds to an estimated macroscopic current density, J_{est} = 4.58 μA/cm^2, where J_{est} = I/A, A = anode-tip area. The anode in our experiment is conical in shape [7] with a tip diameter of 1 mm, so the lines of force emerging from the edge of the anode-tip and terminating to the sample surface are diverging in nature, where as the lines of force emitting from the flat surface are parallel in nature.) were found to be 6 V/μm to 3.6 V/μm for variation of electrode separation (d) = 100 μm to 60 μm. It was also noticed that only bulk-CdS thin films deposited on Si substrate showed no field emission (upto the field applied 30 V/μm; which was our experimental limit). This confirmed that in our case, the field emission property was exhibited due to nanostructured CdS grown in the thin film. So, the 'ENH-material hypothesis' put forward by Forbes [4], that electrically nanostructured heterogeneous (ENH) materials with quasi-filamentary conducting channels inside a less conducting matrix show low-macroscopic field emission, may be applicable to our film also, as nanofibers diameters in the range 2 - 4.3 nm and length a few microns with a film thickness of 200 nm.

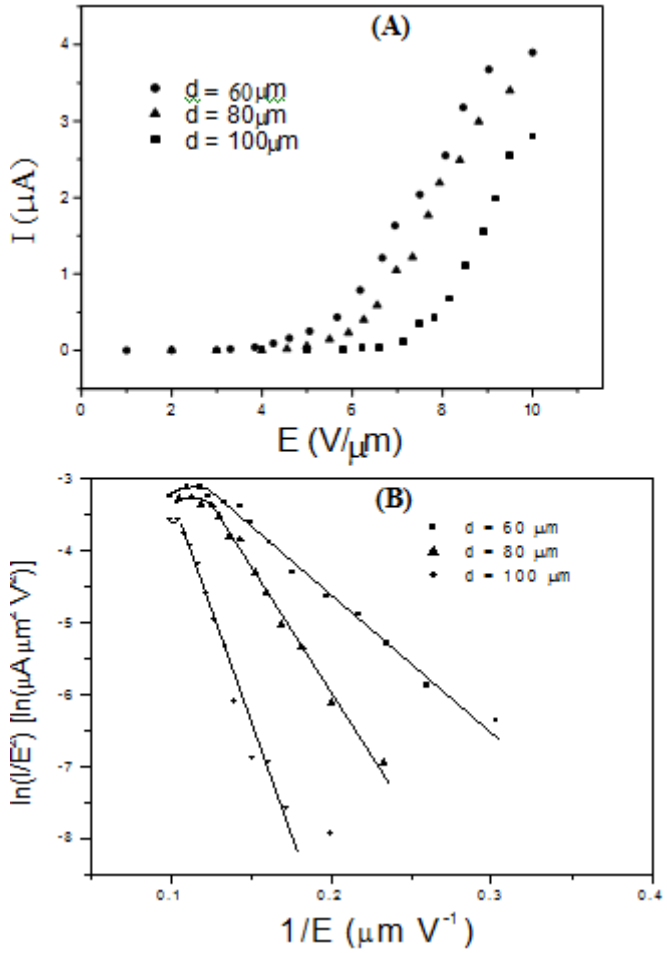

Figure3. *(A) Emission current vs. macroscopic field plot of CdS thin film deposited on Si substrate and (B) Fowler-Nordheim (F-N) plot ($ln(I / E^2)$ vs. $1 / E$ plot).*

According to above equation, the slope of the tangent would carry the information of the local work function (ϕ) of the emitter-tip. Assuming an ideal flat emitter with field enhancement factor (β) equal to 1, we have obtained an estimation of the values of ϕ from the F-N plot lie in the range 2.0713 x 10^{-3} to 4.22 x 10^{-3} eV as obtained from Figure 3(B). But the true local work function must be much larger than these values, due to the factor β, which depends on the shape of the emitter. Forbes [4] determined its value via the 'hemisphere on post approximation' as:

$$\beta \approx \frac{0.7L}{R} \tag{5}$$

β lie within the range 30 ≤ L/R ≤ 2000. (where, L = height of the post, and R = radius of the hemisphere). As the film thickness is ~ 500 nm and the average particle size is as low as ~ a few nm we assume the sharp emission tip radii (R) of our sample of around 20 % to 30 % of the particle size and the height of the post (L) is equal to the film thickness, the approximate β-value of our sample lie in the range 130 to 220. This value of β falls within the range (150 – 300) predicted by Gröning et al [16], for their N-doped diamond like carbon films and they stated that this type of β-values were not unusual even on mirror like polished copper samples. So the local work functions increased by almost two orders of magnitude, and came out in the order of 0.262 to 1.178 eV. It may be mentioned that although bulk CdS is a moderately wide band gap material; but for nano-CdS the band gap increases by more that 1 eV from its bulk value, which essentially behaves as a wide band gap semiconductor. It is also shown (Fig. 2(B)) that the band gaps of CdS nanofibers are indeed quite larger (lie in the range 3.55 eV to 3.76 eV) than that of the bulk value (2.42 eV), and hence the electron affinity of the materials becomes quite low, so the local work function was also low. Actually, the local work function is always less than the true work function of the material because of the enhancement of the local field at the emitter tip.

4. CONCLUSION

TEM and optical studies of CdS nanofibers revealed that the quantum size effect occurred in the films. Field emission study showed the turn on fields are lying in between 3.6 to 6.6 V/μm and the linear F-N plot confirmed the cold field emission of our nanocrystalline thin film. This is also found that the bulk-CdS thin films have showed no field emission at the same conditions. The good field emission properties exhibited by nanocrystalline CdS may give an additional impetus to this already technologically important material.

ACKNOWLEDGEMENT

The author wishes to thank Prof. K. K. Chattopadhyay of Thin Film Nanoscience Laboratory, Jadavpur University Kolkata, for all types of supports during the execution of the work.

REFERENCES

[1] E. N. Wong, P. E. Sheehan, C. M. Lieber, Science 277 **(1997**) 1971.

[2] Q. H. Wang, T. D. Corrigan, J.Y. Dai et al, Appl. Phys. Lett. 70 **(1997)** 3308.

[3] R. G. Forbes, C. J. Edgcombe, U. Valdre, Ultramicroscopy, 95 **(2003)** 57.

[4] R. G. Forbes, Solid State Electron. 45/6 **(2001)** 779.

[5] S. Suresh applied Nanoscience vol. 4 **(2014)** 325-327.

[6] Q. Wan, K. Yu, T. H. Wang, C. L. Lin, Appl. Phys. Lett. 83(11) **(2003)** 2253.

[7] A. N. Banerjee and K. K. Chattopadhyay, Appl. Surface Science 225 **(2004)** 243.

[8] H. Jia, Y. Zheng, X. Chen et al, Appl. Phys. Lett. 82(23) **(2003)** 4146.

[9] J. Chen, S. Z. Deng, N. S. Xu et al, Appl. Phys. Lett. 80(19) **(2002)** 3620.

[10] J. Jiao, L. F. Dong, D. W. Tuggle et al, Mat. Res. Soc.Symp. Proc., 39(H5.4) **(2003).**

[11] X. Ling; H. G. Qi; W. Jian et al, Chinese Physics Letters, 21(10) **(2004)** 2049.

[12] J.C.P.D.S. Powder Diffraction File Card 10 - 454.

[13] Optical Processes in Semiconductors, Pankove, Prentice-Hall.Inc**., (1971).**

[14] E. L. Murphy, R. H. Good Jr., Phys. Rev. 102 **(1956)** 1464.

[15] R. G. Forbes, Ultramicroscopy 79 **(1999)** 11.

[16] O. Gröning, O. M. Küttel, P. Gröning et al, Appl. Phys. Lett. 71 **(1997)** 2253.

Citation: *P. K. Ghosh "The Spectroscopic Studies of CdS Nanofibers Synthesized via Dc-Sputtering Technique", International Journal of Advanced Research in Physical Science (IJARPS), vol. 6, no. 1, pp. 1-6, 2019.*